

## 論文

**MODE I FRACTURE BEHAVIORS OF FRP-CONCRETE INTERFACES**Jianguo DAI<sup>1</sup>, Tamon UEDA<sup>2</sup>, Muttaqin HASAN<sup>3</sup> and Yasuhiko SATO<sup>4</sup>

**ABSTRACT:** The Mode I fracture behaviors of FRP sheet-concrete interfaces are studied by means of conventional three-point bending tests of artificially notched composite beams. Different adhesives and different bonding substrates (concrete and mortar) are used. Based on the test results, the interfacial Mode I fracture energy is evaluated parametrically. And also, the interfacial tension-softening diagram has been derived through Niwa's improved J-integral method and verified through FEM analysis.

**KEYWORDS:** FRP sheet-concrete interface, Mode I fracture, tension-softening diagram, adhesive

**1.INTRODUCTION**

The technology of FRP retrofitting for existing concrete structures together with adhesive bonding system has obtained rapid development in the past decades due to the outstanding advantages of FRP materials. Since the retrofitted structural performances mainly depend on the stress transfer in the adhesive interfaces between FRP and the existing concrete structures, clarifying the interfacial bond mechanisms is one of the most important issues for this technology. In the past a lot of studies on the interfacial shear stress transfer which dominates the special delamination phenomenon (so called Mode II interfacial fracture) have been carried out by many research groups including the authors'. Correspondingly different types of interfacial shear bond stress-slip constitutive models have been proposed. However, as far as the authors' reviewed literatures are concerned, there are very limited literatures concerning another type of interfacial fracture named as interfacial Mode I fracture and almost no literature has dealt with the interfacial tension softening behaviors, which can be described by using the stress-crack width relation according to the Hilliberg's fictitious crack method. Meanwhile, unsimilar to the pure shear bond test, no test method for Mode I interfacial fracture has been accepted as a common one.

In fact, the more representative interfacial fracture may be a mix mode one in FRP retrofitting concrete structures. That can be caused by the relative displacement parallel to concrete cracks, the deformation differences among the dissimilar interfacial materials due to shrinkage or temperature effects, the localized stress concentration at cutoff points of FRP materials and so on. In FRP strengthened beam cases, this mix-mode delamination failure at the cutoff points of FRP materials or near the shear-flexural cracks has been widely reported [1-3]. Moreover, in some cases of retrofitting curved concrete structures, such as tunnel lining, the mode I interfacial fracture may become dominant. So it is necessary to understand two different fracture mechanisms parametrically and quantify both components of interfacial fracture energy, upon which an overall interfacial fracture model can be proposed.

**2.TEST PROGRAM****2.1 Test setup**

To get the Mode I interfacial fracture energy and characterize the softening behaviors of a material in tension, the most straightforward way is to perform uni-axial tension tests under closed-loop displacement control. However, such a test procedure is complicated to carry out in comparison with bending tests. So conventionally for concrete, the three point bending test for a notched beam is recommended by RILEM [4] to evaluate the Mode I fracture energy. In the present study, the method is modified to test the Mode I fracture energy and tension softening behaviors of FRP sheets concrete interfaces as shown in Fig.1. The procedures for preparing the composite specimens including the FRP sheet-interface are:

- 
- 1.Division of Structural and Geo-technical Engineering, Hokkaido University, Dr. E., Member of JCI
  - 2.Division of Structural and Geo-technical Engineering, Hokkaido University, Dr. E., Member of JCI
  - 3.Division of Structural and Geo-technical Engineering, Hokkaido University, M. E., Member of JCI
  - 4.Division of Structural and Geo-technical Engineering, Hokkaido University, Dr. E., Member of JCI

- (1) Preparing two parts of concrete specimens with the size of 10×10×20cm;
- (2) Processing the bonding surfaces of two concrete specimens then covering with primer;
- (3) Adhering FRP sheet on one of the two concrete specimens to make the possible fracture happen in one of the two FRP-concrete interfaces.

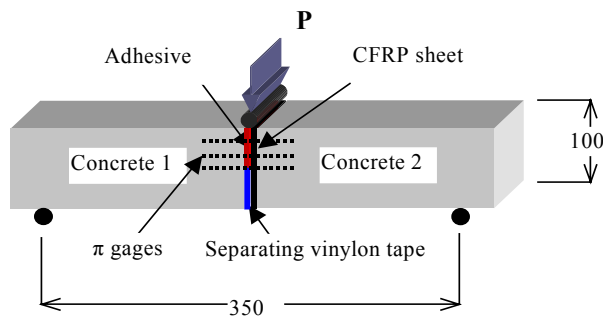


Fig.1 Configuration of test specimens

- (4) Conjuncting the two parts of concrete with adhesives. Half height (5cm) of the connected interface is separated with several layers of vinylon tapes to induce the notch.

To obtain the crack tip open displacement (*CTOD*) as well as the crack propagation process three  $\pi$  gages with the accuracy of 0.001mm were arranged with the same distance from the position of crack tip to the top of composite beam. All the specimens are tested under the displacement controlled cyclic loading condition. The loading speed is 0.1mm/min.

## 2.2 Experimental materials

It was observed in the authors' previous studies that modifying the mechanical properties of adhesive bond layer can improve the Mode II interfacial fracture energy significantly. So four types of adhesives besides the primer (*FR-E3P*), which are same as that used previously [5], are applied presently. These materials have different stress-strain relations as shown in Fig.2. Due to the obvious non-linearity with the adhesive, the initial elasticity modulus is defined as the average secant modulus when the strain lies between 0.0005 and 0.0025. [6] The material properties of adhesives and FRP are indicated in Table.1. Two types of bonding substrates, concrete (*C1*, *C2* series) and mortar (*MI* series) are prepared to simulate the actual bonding situation in real retrofitting fields. The *W/C* ratio for concrete *C1* and *C2* series are 0.5 and 0.4 respectively and the strength properties of concrete and mortar can be found in Table.2.

Table 1 Material properties of adhesive and FRP

Types of materials		Tensile strength (MPa)	Shear strength (MPa)	Elasticity modulus (MPa)
Adhesive*	FR-E3P (R1)	44.7	--	2405
	SX-325 (R2)	15.9	23.6	999
	CN-100 (R3)	11.8	14.6	390
	EE-50 (R4)	>2	--	3
	FP-NS (Primer)	48.1	--	2455
CFRP*	FTS-C1-20	3500	--	230×10 <sup>3</sup>

Note: Except that adhesive EE-50 was tested by Toho Co. Ltd., the others were tested by Sho-bond Co. Ltd according to JIS K7113 [6]. CFRP is from Nippon Steel Composites Co. Ltd.

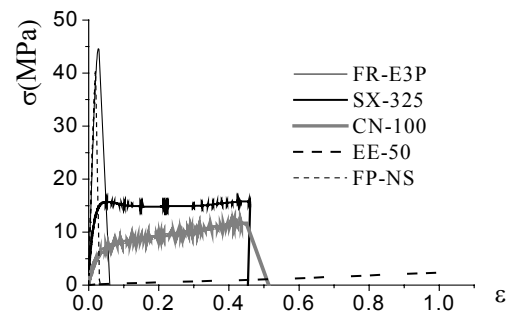


Fig.2  $\sigma$ - $\epsilon$  curves of adhesives

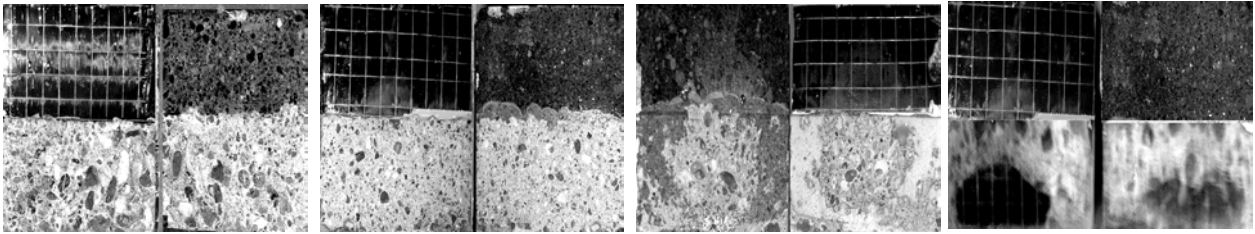
## 3. TEST RESULTS AND DISCUSSION

### 3.1 Failure mode description

Fig.3 show the observed several types of fractured interfaces. In common, most of the specimens fracture at the concrete (mortar) side of the interfaces (See Fig.3.a-Fig.3.c). Only in one specimen, the interfacial fracture propagates partially into the interface between FRP and adhesive (See Fig.3.d). In comparison with the concrete interface (see Fig3.a), the fractured mortar surface is more even (See Fig.3.b). It can be distinguished by naked eye that the volumes of the fractured concrete attached to adhesive side are different. Especially, in comparison with other adhesives, when the softest adhesive *EE-50* is used, obviously less concrete volume attaches to the adhesive side (see Fig.3.c) and the maximum bending force is lower correspondingly (See specimens *C1-R4-1* and *C1-R4-2* in Table.2).

In Mode II fracture tests of FRP sheets-concrete interfaces it is well known that the fracture of interface always happens in a thin concrete layer just beneath the adhesive layer. And also it was observed there exists a thin interlocking mortar layer (primer penetrating into the pore structures of concrete) between the adhesive layer and concrete layer. For different adhesives and FRP stiffness, the critical interfacial shear

stresses of bond layer show significant differences. In the present Mode I test, the similar cohesion failure happens within the concrete mostly near the interface as shown in Fig.3. In order to verify whether the



interfacial peak stress under Mode I fracture is determined by the tensile strength of concrete or by that of the special transition layer, another subsidiary direct tension pullout test was carried out (See Fig.4). The section area of concrete bonding with adhesives is 4×4cm[7]. The concrete substrate with some artificial grooves, of which the depth is more than 2cm to ensure the uniform tensile condition [8], is made of the fractured beams after the bending test. It is somehow surprisingly found that all the fracture under the direct pullout test happens far away from that interlocking layer regardless of adhesive types as shown in Fig.4 (*FR-E3P* and *EE-50* are used in the left and right specimens respectively). This indicates the Mode I interfacial peak strength can be determined based on the concrete tensile strength uniquely if the tensile strength of adhesive is stronger than that of concrete. Comparing the pullout tensile and the splitting tensile strength, it is found that the pull-out tensile strength of the concrete is significantly lower than the splitting tensile strength (See  $f_{split}$  and  $f_{pull}$  in Table.2). Comparatively, both two strengths show similar values in the cases of using mortar-bonding substrates (See *MI-R1* and *MI-R3* in Table 2). This can be considered as the effects of aggregate size. In the present study, the maximum diameter of coarse aggregates is 2.0cm, which is closely to the size of bond interfaces (4×4cm). From this viewpoint, it can be said that this type of direct pullout test for FRP-concrete interface is not a reliable way to determine the interfacial strength but a practical way to evaluate the interface qualitatively.

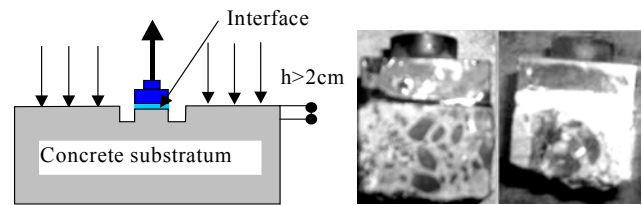


Fig.4 Direct pull-out test of adhesive-concrete interfaces

### 3.2 Mode I Fracture energy of the interfaces

Table.2 shows all Mode I fracture test results of the FRP-concrete interfaces. The Mode I interfacial fracture energy  $G_{f,I}$  is calculated based on the experimental load displacement curves using RILEM recommended expressions [4]. The average  $G_{f,I}$  value of all specimens is 141.1N/mm, which has big difference with the value of 410N/mm reported by V.M.Karbhari et al. [9], who applied a special peeling angel adjustable interfacial fracture test method. The comparison indicates that test method greatly affects the determination of the Mode I fracture energy of FRP-concrete interfaces. Fig.5 shows the values of  $G_{f,I}$  affected by the

Table. 2 Interfacial Mode I fracture test results

Specimen codes	$G_{f,I}$ (N/m)	$P_{max}$ (kN)	$\delta_{max}$ (mm)	CTOD <sub>max</sub> (mm)	$f'_c$ (MPa)	$f_{split}$ (MPa)	$f_{pull}$ (MPa)	Failure mode
C1-R1-1*	147.1	2.55	1.755	0.375				a*
C1-R1-2	136.5	2.52	0.950	0.492				a
C1-R2-1	123.9	2.69	0.821	0.413				a
C1-R2-2	169.7	2.94	1.241	0.587	43.0	4.41	2.86	a
C1-R3-1	182.0	3.18	1.046	0.498				a
C1-R3-2	196.6	3.18	1.260	0.638				a
C1-R4-1	187.3	1.70	1.717	0.752				b
C1-R4-2	161.4	1.78	1.476	0.698				b
C2-R1-1	116.9	3.13	0.777	0.354				a
C2-R1-2	109.6	2.70	0.730	0.352	49.6	4.67	3.23	a
C2-R3-1	141.4	2.87	0.806	0.355				a
C2-R3-2	147.5	2.80	1.338	0.657				d
M1-R1-1	108.4	2.55	1.232	0.610				c
M1-R1-2	105.8	2.17	0.738	0.351	39.6	4.34	4.07	c
M1-R3-1	118.1	2.39	0.895	0.418				c
M1-R3-2	95.7	2.20	0.930	0.465				c

Note: R1, R2, R3 and R4 mean adhesive FR-E3P, SX-325, CN-100 and EE-50 respectively. Failure mode a, b, c and d correspond Fig.3.a, b, c and d.  $G_{f,I}$ : Mode I fracture energy;  $P_{max}$ ,  $\delta_{max}$ , CTOD<sub>max</sub>: the maximum bending force and corresponding mid-span deflection and CTOD;  $f'_c$ ,  $f_{split}$ ,  $f_{pull}$  the compressive, the splitting tensile (cylinder) and the direct pull-out tensile strength of concrete.

adhesives and different bonding substrates. Based on the figure and the Table 2, the experimental observations in this study can be summarized as follows:

(1) Concrete series *C1* shows obviously higher values of  $G_{f,I}$  in comparison with the mortar series *M1* though they have similar splitting tensile strength. This is because that mortar has less bridging effects due to the lack of coarse aggregates. While in Mode II interfacial fracture test the fracture energy  $G_{f,II}$  does not show noticeable differences between concrete and mortar substrates [10].

(2) The  $G_{f,I}$  value has almost no change when the adhesive changes from the normal one *FR-E3P* (with elasticity modulus of  $2.4GPa$ ) to *SX-325* (with elasticity modulus of  $1.0GPa$ ). While with the further decreasing of the elasticity modulus of adhesives to *CN-100* (with elasticity modulus of  $0.39GPa$ ), in both *C1* and *C2* concrete series,  $G_{f,I}$  shows increasing tendency. Comparatively in mortar *M1* series,  $G_{f,I}$  shows almost no change. As shown in Fig.2, the adhesive *CN-100* shows significant non-linearity and good toughness at lower tensile stress level, which can lead to higher interfacial energy consumed during the whole fracture process. Whereas interfacial deformation accumulated in the adhesive layer with higher elasticity modulus before the interfacial peak stress will be released almost thoroughly. Comparing with the effects of adhesives on Mode II fracture energy the effects on  $G_{f,I}$  are less remarkable, because the values of  $G_{f,II}$  in the case of using *CN-100* in the adhesive layer was above doubled than that in the case of using *FR-E3P* according to the previous studies of the authors [5].

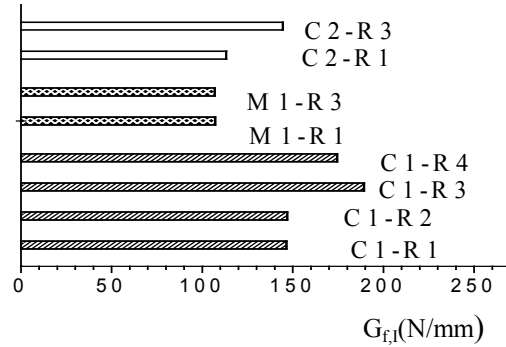


Fig5  $G_{f,I}$  of FRP-concrete interfaces

(3) The concrete series *C2* shows lower values of  $G_{f,I}$  in comparison with concrete series *C1* although their strength is higher than that of *C1* series. Whereas, it is generally reported by most of researchers that the Mode I fracture energy increases with the strength of concrete. Uchida et al. [11] observed that the fracture energy decreases with increasing concrete strength in their studies. They think that the bridging effects of aggregates become weaker as the strength increases because the crack surface becomes plane due to the higher mortar's strength. In this study, it is considerable that the value of  $G_{f,I}$  is more sensitive to the proportion of fine aggregates near the interface because the fracture always happens mostly near to the interface. During the casting procedures of *C2* series, no strong vibrating was exerted due to the high flowability. That may affect the distribution of aggregates near the interface. Unfortunately, the strength difference between *C1* and *C2* is not remarkable enough in the present study. So more experiments should be carried out to clarify the concrete properties' effects on the  $G_{f,I}$  of FRP-concrete interfaces.

#### 4.CONSTITUTIVE MODEL FOR MODE I INTERFACIAL FRACTURE AND VALIDATION

To get the tension-softening diagram after the interfacial peak stress, Niwa et al. proposed a modified

J integral method, which can consider the propagation of the crack length and remove the elastic displacement of the beam due to the crack [12]. As shown in Fig.6, the J-integral is defined as the energy available for crack extension and can be interpreted as the total absorbed energy of the cracked specimens minus its elastic energy as follows:

$$J = \frac{1}{ab} \left[ \int_0^\delta P(\delta) d\delta - \frac{1}{2} P(\delta)(\delta - \delta_p) \right] \quad (1)$$

The cohesive stress-crack relation can be obtained as:

$$\sigma(w) = 2 \frac{dJ}{dw} + w \frac{d^2 J}{d^2 w} \quad (2)$$

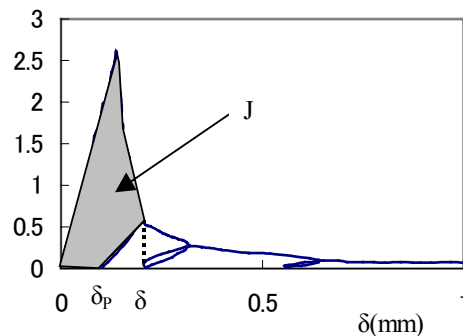


Fig.6 Improved J integral method based on P- $\delta$  curve

where  $b$  is the width of beam, the crack propagation length  $a$  corresponding to a crack width can be recorded through the arranged three above mentioned  $\pi$  gages (see Fig.1) and the plastic deformation  $\delta_p$  of beam is obtained through unloading and reloading as shown in Fig.6.

Fig.7 shows the experimental  $\delta$ - $\delta_p$  relations (normalized by the maximum deflections). Despite of the existence of the data scattering, it can be seen the  $\delta$ - $\delta_p$  relation for FRP-concrete interfaces is almost same as that proposed by Niwa et al. for ordinary concrete regardless of the adhesive types.

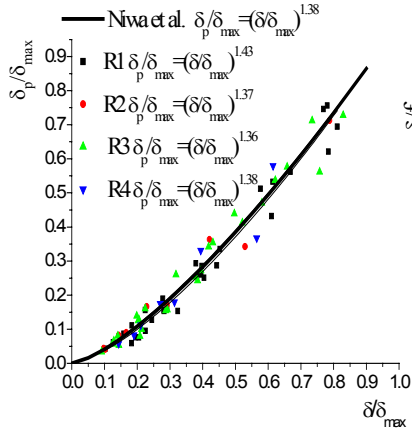


Fig.7  $\delta_p/\delta_{max} \sim \delta/\delta_{max}$  relation

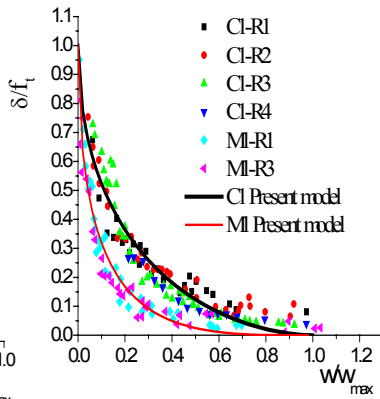


Fig.8  $\sigma \sim w$  relations of C1 and M1 series

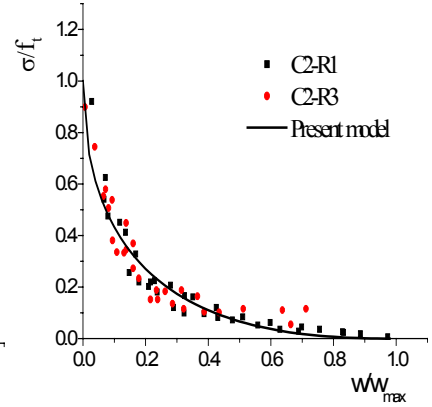


Fig.9  $\sigma \sim w$  relations of C2 series

The  $\sigma \sim w$  relations for all specimens can be obtained as shown in Fig.8 and Fig.9, where the interfacial cohesive stresses are normalized by the interfacial tensile strength and the crack width is normalized by the estimated maximum crack width. The interfacial tensile strength is taken from the concrete splitting tensile strength because the direct pullout strength shows lower value due to the effects of tensile section area mentioned above. In addition, it is reported that the modified integral method may give rather ductile  $\sigma \sim w$  curves [12]. Therefore, in this study the maximum crack widths in the cases of different adhesives and bonding substrates are determined to get rather better fitting for the beginning part of tension softening curves, which is more important for the interfacial simulation. It can be seen from Fig.8 that the mortar bonding substrate shows fragile tension softening behaviors, which lead to smaller interfacial Mode I fracture energy as discussed previously. According to the way of normalization, all the tension softening curves can be expressed as the following one:

$$\alpha \sqrt{\frac{\sigma}{f_t}} + \sqrt{\frac{w}{w_{max}}} = 1 \quad (3)$$

where  $\alpha$  is taken as 3.0, 2.5 and 2.2 for *M1*, *C2* and *C1* series respectively.  $w_{max}$  is taken as 0.30mm for both concrete and mortar bonding substrates in the case of using higher elasticity modulus adhesives ( $E_a$  higher than 0.9GPa in this study), whereas 0.34mm in the cases of using lower elasticity modulus adhesives ( $E_a$  less than 0.5GPa in this study).

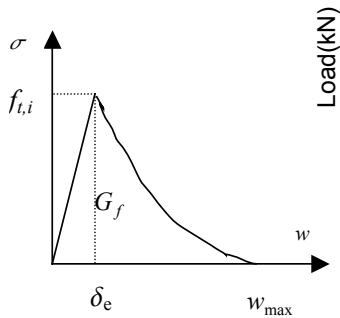


Fig.10 Interfacial constitutive model

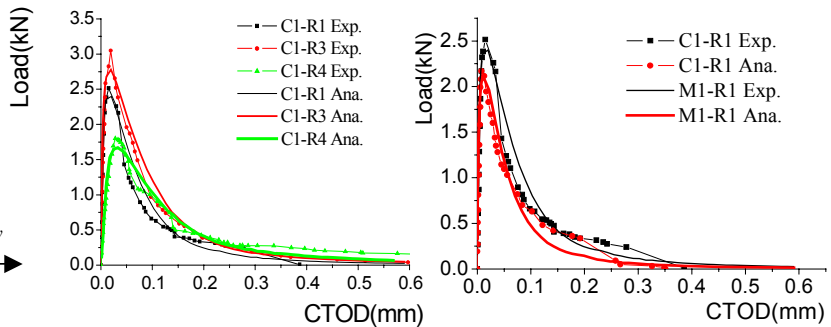


Fig.11 The experimental and analytical load-CTOD relations

$$\sigma = \frac{E_a}{t_a} \delta, \delta \leq \delta_e = \frac{f_{t,i}}{E_a} t_a \quad (4)$$

$$\sigma = f(w) (Eq.3), \delta_e < \delta \leq w_{max} \quad (5)$$

$$\sigma = 0, \delta > w_{max} \quad (6)$$

The constitutive model for the Mode I fracture of FRP-Concrete interfaces can be described as shown in Fig.10 and the corresponding expressions are written as Eq.4~Eq.6. Then the interfacial constitutive model is implemented into FEM analytical program [13], where the eight-node isoparametric elements are employed to model the concrete and the six-node non-thickness interface elements are used to model the FRP-concrete interfaces. Fig.11 show the acceptable accordance between the experimental and analytical results, indicating the validation of the proposed constitutive model.

## 5.CONCLUDING REMARKS

Based on above experimental and analytical studies, some conclusions can be drawn up as follows:

(1) Three point bending test method can be applied to evaluate the interfacial Mode I fracture of FRP-concrete interfaces bonded with adhesives. The interfacial tension-softening diagram can be derived as well based on the modified J-integral method developed for ordinary concrete.

(2) Unsimilar to their effects on the mode II interfacial fracture energy, the adhesives have fewer effects on the interfacial Mode I fracture one. However, when the adhesive shows good toughness under low stress-level, the Mode I fracture can be improved even though the fracture happens always in concrete mostly near the interface and the interfacial peak strength is proved to be determined by concrete strength.

(3) The Mode I fracture energy relies greatly on the quality of bonding substrates. Mortar and concrete surface causes significant difference even their tensile strengths are similar.

(4) For the numerical simulation of FRP-concrete interfaces, the open displacement between FRP and concrete can be simulated as a fictitious crack. An interfacial Mode I fracture model is proposed and verified through FEM simulation.

## ACKNOWLEDGEMENT

The authors would like to give sincere thanks to Dr.SHIMURA Kazunori and Dr.TAKANO Tomohiro, Hokkaido University for their helps during experiments.

## REFERENCES

1. Buyukozturk, O. and Hearing, B., "Failure Behaviors of Precracked Concrete Beams Retrofitted with FRP", *Journal of Composites for Construction*, Vol.2, No.3, 1998,pp.138-144
2. R.N.Swamy, "Debonding of Carbon-fiber-reinforced Polymer Plate from Concrete Beams", *Proc. Instn Civ. Engrs Structus & Blds*, 134, Nov., 1999, pp.301-317
3. Hamid Rahimi and Allan Hutchinson, "Concrete Beams Strengthened with Externally Bonded FRP Plates", *Journal of Composites for Construction*, Vol.5, No.1, 2001, pp.44-56
4. RILEM Draft Recommendation (50-FMC), "Determination of the Fracture Energy of Mortar and Concrete by Means of Three Point Bend Tests on Notched Beams, *Materials and Structures*", Vol.18, No.106, 1985, pp.287-297
5. Dai Jianguo, Yasuhiko Sato and T. Ueda, "Improving the Load Transfer and Effective Bond Length for FRP Composites Bonded to Concrete", *Proceedings of the Japan Concrete Institute*, Vol.24, 2002, pp.1423-1428
6. JIS K7113-1995, "Testing Method for Tensile Properties of Plastics"
7. JIS A 6909-2000, "Coating Materials for Textured Finisher of Buildings"
8. Simon Austin, Peter Robins and YouGuang Pan, "Tensile Bond Testing of Concrete Repairs", *Materials and Structures*, Vol.28, 1995, pp.249-259
9. V.M.Karbhari and M.Engineer, "Investigation of Bond between Concrete and Composites: Use of a Peel Test", *Journal of Reinforced Plastics and Composites*, Vol.15, Feb., 1996, pp.208~227
10. K., Nakaba et al., "Bond Behavior between Fiber-Reinforced Polymer Laminates and Concrete", *ACI Structural Journal*, V.98, No.3, 2001, pp.359-167.
11. Y.Uchida et al., "Tension Softening Curves of Concrete Determined from Different Test Specimen Geometries", *FRAMCOS-3*, 1998, pp.387-398
12. J.Niwa et al., "New Method to Determine the Tension Softening Curve of Concrete", *Fracture Mechanics of Concrete Structures*, *Proceedings of FRAMCOS-3*, 1998, pp.347-356
13. WCOMR FEM analytical program (modified version by Hokkaido university)